

# Mechanical properties of transparent functional thin films for flexible displays

Y. Leterrier<sup>1</sup>, C. Fischer<sup>1,3</sup>, L. Médico<sup>1</sup>, F. Demarco<sup>1</sup>, J.-A. E. Månson<sup>1</sup>, P. Bouten<sup>2</sup>, J. DeGoede<sup>2</sup>, J.A. Nairn<sup>3</sup>

(1) Laboratoire de Technologie des Composites et Polymères (LTC)

Ecole Polytechnique Fédérale de Lausanne (EPFL), CH 1015 Lausanne, Switzerland

(2) Philips Research Laboratories, Prof. Holstlaan 4, 5656 AA, Eindhoven, The Netherlands

(3) University of Utah, Materials Science and Engineering

122 S Central Campus Dr Rm 304, Salt Lake City UT 84112-0560, USA

---

**Key Words:** Flexible polymer-based displays  
Transparent conductive coatings

Permeation barrier coatings  
Adhesion

---

## ABSTRACT

The present work investigates the mechanical integrity of multilayer films developed for flexible displays. The layers comprise tin-doped indium oxide (ITO) conductive coatings and alumina barrier coatings sputtered onto high temperature aromatic polyesters. The onset strain for tensile failure and related cohesive strength of the coatings, and their adhesion to the polymer substrate, are analyzed by means of bending tests and fragmentation tests. The former test enables accurate electrical resistivity measurements during bending of film specimens, and correlates the failure of the ITO coating to the abrupt increase of resistivity. In the fragmentation test, the progressive failure of the thin coating is examined in situ in an optical microscope as a function of tensile strain, with simultaneous measurement of the electrical resistance, for the ITO coatings. The results and their analysis provide accurate determination of the influence of internal stresses and layer thickness on the failure mechanisms of the multilayer composite films.

## INTRODUCTION

Color displays based on organic light emitting devices (OLED) deposited onto flexible substrates are being developed as alternatives to liquid crystal displays (LCD) [1]. Substrates for flexible OLED are multilayer composite structures comprising a polymer-based substrate on which are deposited a moisture barrier layer and a transparent conducting coating used to address image pixels. The maximum achievable bending and reliability of the display is dictated by the fracture properties of these extremely thin and brittle films, controlled by a complex interplay between process induced defects and residual film stresses, cohesive properties and adhesive properties of the individual layers [2].

A rigorous analysis of the damage evolution of these coatings under mechanical load requires accurate and simultaneous measurement of strain and detection of cracks in the coating. In addition, measurements of stress and of the electrical properties of the ITO can be useful. Electrical resistivity measurements used in recent studies of conductive coatings revealed the existence of a thickness dependent critical strain, when the resistance started to increase abruptly when the conductive layer failed mechanically [3; 4; 5]. However, these works ignored compliance phenomena, leading to unknown overestimations of critical strains. More, process-induced internal stresses, known to change to a considerable extent the hardness, coefficient of friction, and practical adhesion of ITO coatings on glass [6], were not accounted for, which prevents a proper analysis of the cohesive and adhesive properties of the materials.

The objective was first to establish reliable mechanical test methods, to investigate the failure mechanisms of the brittle thin films on polymer substrates. A second objective was to determine the influence of internal stresses and coating thickness on these failure mechanisms. These informations should be useful for accurate mechanical simulations, for example of crack initiation and growth under complex thermomechanical cycles, to eventually enable optimal design of OLED structures.

## EXPERIMENTAL

### Materials

Two types of multilayer composite films were analyzed, namely alumina ( $Al_2O_3$ ) coated barrier films, and ITO coated conductive films, as summarized in Table I. In both cases, the substrate was a high temperature aromatic polyester (ARY) coated on both sides with a silica-epoxy hybrid solvent barrier (HC/ARY/HC).

**Table 1. Multilayer composite structures.**

Multilayer barrier structures	
BAR1	Al <sub>2</sub> O <sub>3</sub> (60 nm)/HC/ARY/HC
BAR2	Al <sub>2</sub> O <sub>3</sub> (60 nm)/UVA (300 nm)/HC/ARY/HC
BAR3	Al <sub>2</sub> O <sub>3</sub> (60 nm)/UVA (300 nm)/Al <sub>2</sub> O <sub>3</sub> (60 nm)/HC/ARY/HC
Multilayer conductive structures	
ITO50	ITO (50 nm)/HC/ARY/HC
ITO100	ITO (100 nm)/HC/ARY/HC
ITO200	ITO (200 nm)/HC/ARY/HC

**The bending test**

In the bending test, originally developed to determine the critical failure strain of optical fibers [7] and extensively described in ref. [8], a rectangular film sample is loaded between parallel plates, with the lowest radius of curvature  $R_{min}$  and the largest (tensile) strain  $\epsilon_{max}$  at the (outer) surface in the middle of the bent (Figure 1). Assuming a purely elastic deformation, one has  $\epsilon_{max} = 1.198 h/L = h/2R_{min}$ , where  $h$  is the sample thickness and  $L$  is the distance between the neutral lines ( $L_0 = L+h$  is the plate distance). The device allows the measurement of electrical resistance  $R$  (two-point method) during loading the sample. When the ITO layer fails, the initial resistance  $R_0$  increases, and a critical strain was defined as the strain  $\epsilon_{max}$  where the relative resistance increase  $R/R_0$  was equal to 10%. Although the bending test is limited to conductive coatings, it does not require compliance corrections, and is moreover fast and easily automated.

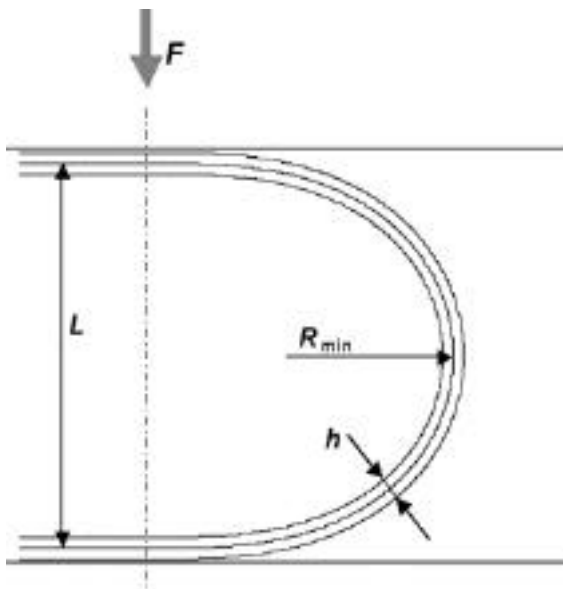


**Figure 1.** Geometry of the substrate (thickness  $h$ ) in the bending test.

**The fragmentation test**

In the fragmentation test, the evolution of crack patterns in the brittle coating is monitored as a function of the uniaxial tensile load applied to the substrate [9]. Tests were carried out in-situ in an optical microscope, using a computer-controlled tensile frame equipped with contactless video extensometry, that overcome compliance effects, and special clamps to enable two-point electrical resistance measurements (Figure 2). The coating strain at failure (and related cohesive properties) was measured with an accuracy better than  $10^{-3}$ , and, in case of ITO coatings, compared to the critical strain determined from the resistance measurements, using the same 10% increase criteria as in the bending test. The coating/substrate adhesion, usually represented by the interfacial shear strength (IFSS, a practical determination of adhesion), was related to the density of coating cracks, measured in the saturation stage of the fragmentation process, i.e., when no more cracks are formed as the strain is increased. The fragmentation test is not limited to conductive coatings and provides useful insight into the damage processes of the thin oxide layers, but is more time consuming than the bending test.

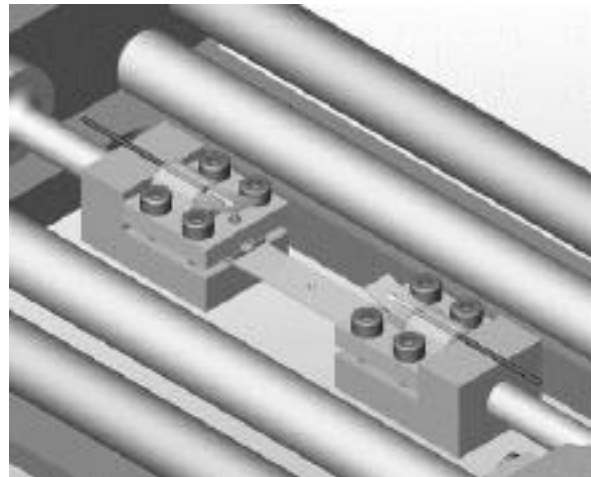


**Figure 2.** Tensile frame with modified clamps for testing conductive coatings.

**Internal stresses**

Process-induced internal stresses were determined from radius of curvature measurements, following the analysis of Röll [10]:

$$\epsilon_i = -\frac{E_s h_s^2}{6(1 - \nu_s) h_c} \left[ 1 + \frac{h_c}{h_s} \left( 4 \frac{E_c}{E_s} - 1 \right) \right] \left( \frac{1}{R_2} - \frac{1}{R_1} \right) \quad (1)$$

where  $E_s$  and  $E_c$  are the Young's moduli of the substrate and coating, respectively,  $h_s$  and  $h_c$  are the corresponding

thickness, and  $R_1$  and  $R_2$  are the radii of curvature of the coated and uncoated substrates. The usual convention, where compressive stresses are negative, was adopted.

### FAILURE ANALYSIS OF BARRIER FILMS

A limited amount of compressive stresses build up in the  $Al_2O_3$  layer during sputtering, found to be equal to  $575 \pm 232$  MPa in the BAR1 structure. Figure 3 shows the tensile failure process of the  $Al_2O_3$  and HC layers in structures BAR1, BAR2 and BAR3, together with that of the uncoated HC/ARY/HC film, in terms of crack density vs. strain. No cracks were detected in the UVA layer. A careful examination of these results reveals three main features.

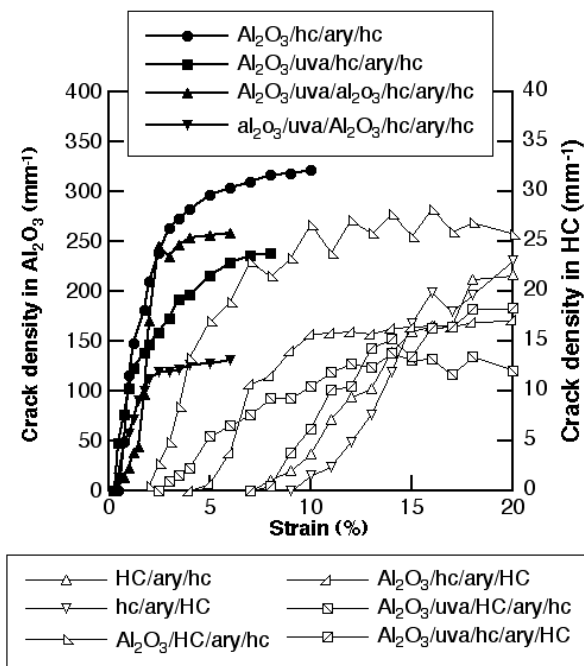


**Figure 3.** Crack density in  $Al_2O_3$  (filled symbols; left axis) and in HC (open symbols; right axis) layers in multilayer barrier structures vs strain. Layers are identified in the legends in uppercase letters.

Firstly, the crack onset strain (COS) of the  $Al_2O_3$  layer is the same within experimental scatter, whatever the multilayer structure, and found to be equal to 0.75%, which corresponds to a minimum achievable radius of curvature of approx. 7 mm. This result also indicates that internal stresses in the  $Al_2O_3$  are comparable in the four types of  $Al_2O_3$  layers [11].

Secondly, the crack density at saturation ( $CD_{sat}$ ) of the  $Al_2O_3$  layer is strongly dependent of the type of multilayer

structure. This result suggests different IFSS between the alumina and the UVA or HC substrates.

Thirdly, the failure onset of the HC layer (approx. 8%) is considerably reduced in presence of an  $Al_2O_3$  layer (down to 2%), a consequence of the following coupling phenomena, illustrated in Figure 4 for the BAR1 structure. A crack in the  $Al_2O_3$  layer locally induces a stress concentration in the underlying HC layer, thus lowering its strain to failure. Cracking of the HC relaxes the axial stress in the  $Al_2O_3$  in the vicinity of the crack, and the resulting exclusion zone prevents further cracking of the oxide. As a consequence, the measured crack density is reduced, hence the IFSS derived from the  $CD_{sat}$  following the standard stress transfer approach detailed in the ref. [9], is underestimated and should be considered as a lower bound. Following this simplified approach, the IFSS between  $Al_2O_3$  and HC was found to be equal to 81 MPa, significantly larger than that between the  $Al_2O_3$  and UVA, found to be equal to 54 MPa. These values were calculated based on an elastic modulus and cohesive strength of the alumina respectively equal to 400 GPa and 3 GPa.

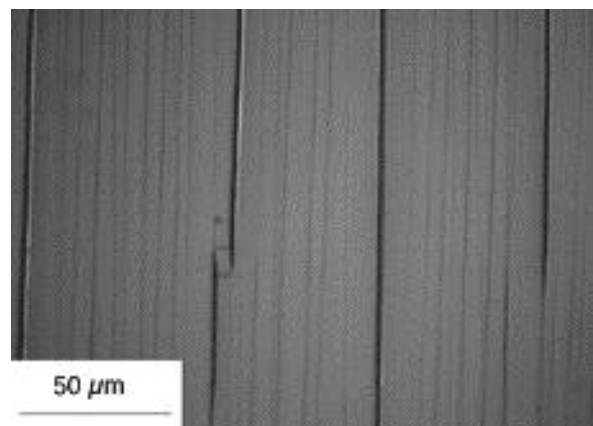


**Figure 4.** Crack patterns in a 60 nm thick  $Al_2O_3$  film (thin cracks) and the underlying hard coat layer (thicker, dark cracks), under 5.15% strain.

Numerical simulations of the failure processes in these layered composite structures are required and are in fact currently being carried out, in order to resolve the coupling phenomena and derive accurate IFSS, coating and interface toughness.

### FAILURE ANALYSIS OF CONDUCTIVE FILMS

The failure of the 100 nm thick ITO coating on the polymer (ITO100 structure) under 1.4% and approx. 5% uniaxial tensile strain is shown in Figure 5. As grown ITO is characterized by a distribution of microdefects in form

of pin-holes produced during coating deposition, and surface defects of the underlying polymer substrate. Upon loading, the very initial cracks originate at defect sites and propagate to span the whole sample width. The normalized resistance increase during the early stages of the fragmentation process, measured during bending and tensile loading, is reported in Figure 6 for a number of ITO100 samples, and the critical strains are reported in Table 2 for the three structure studied. The onset of tensile failure is detected at the same strain for the two types of measurement techniques. It is moreover evident that the thinner ITO coatings fail at a higher strain than thicker ones.

At higher strain, the HC layer fails (Figure 5), as was pointed out in case of the barrier multilayer structures. Again, solving of the resulting coupling process requires numerical methods, in order to derive accurate adhesion values.

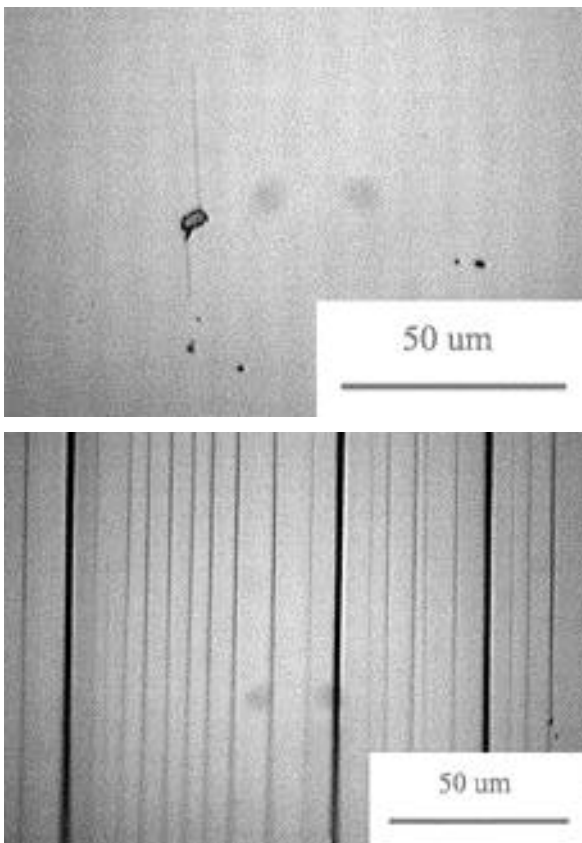


**Figure 5.** Crack initiation in ITO on pin-holes at 1.4% strain (top), and simultaneous failure of the ITO and top HC layer at 5% strain (dark crack features; bottom).

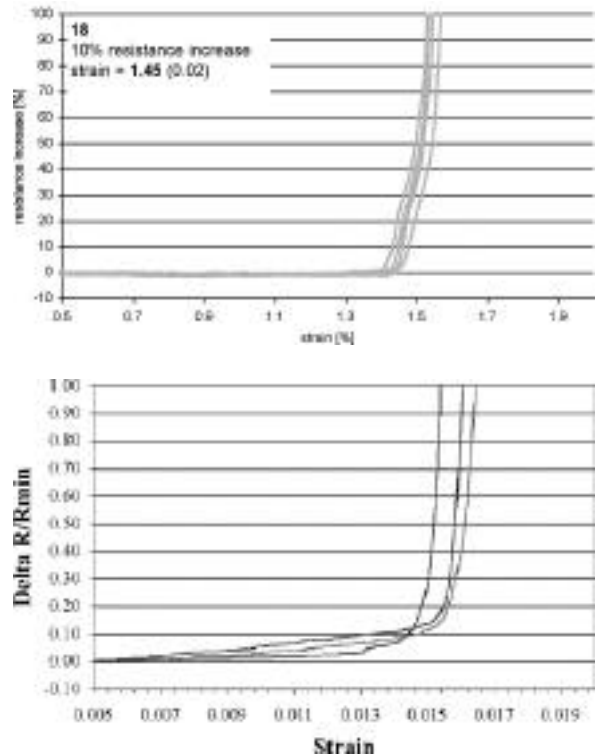


**Figure 6.** Normalized resistance change during bending (top) and tensile (bottom) loading of 100 nm thick ITO coatings, in the vicinity of the critical strain for failure.

**Table 2. Crack onset strains (COS) of ITO layers.**

ITO thickness (nm)	Bending R/R <sub>0</sub> =10%	Tensile R/R <sub>0</sub> =10%
50	1.77±0.03	1.82±0.07
100	1.45±0.02	1.42±0.15
200	1.56±0.03	1.45±0.16

**Influence of ITO thickness on crack onset strain**

As grown ITO coatings are systematically under compressive stress [12], with stress levels that increase with ITO thickness. Figure 7 depicts the influence of coating thickness on internal stress and crack onset strain (COS) for as-grown ITO coatings. The minimum achievable radius of curvature for the 50 nm thick ITO coated film is close to 3 mm, and it is approx. equal to 3.5 mm for both the 100 nm and 200 nm thick ITO layers. Interestingly, the COS does not decrease with thickness as would be expected from classic analyses [13]. The reason is the presence of internal stresses that influence the strain at failure following:

$$COS = COS^* - i \tag{2}$$

Where  $\text{COS}^*$  represents the intrinsic crack onset strain,  $\epsilon_i = \sigma_i(1 - \nu_c)/E_c$  is the internal strain ( $\sigma_i$  being the internal stress,  $\nu_c$  and  $E_c$  the ITO Poisson's ratio and Young's modulus, respectively assumed to be equal to 0.2 and 100 GPa). In other words, an internal compressive strain (negative by convention) is beneficial since it increases the net strain for tensile failure of the coating. It is evident that internal stress increases with ITO thickness. In contrast, the  $\text{COS}^*$  decreases with increasing ITO thickness. Whereas no model seems to exist to describe the thickness dependence of the internal stress, a number of approaches have been proposed in previous works to analyze the defect-controlled cohesion of brittle phases in composite materials. These approaches are based on fracture mechanics, and, assuming a linear elastic behavior, lead to the classic scaling [13; 14]:

$$\text{COS}^* \propto h_c^{-1/2} \quad (3)$$

This scaling reproduces within experimental scatter the  $\text{COS}^*$  data of as-grown ITO coatings shown in Figure 7.

This analysis enables to determine the respective influence of internal stresses and layer thickness on the failure mechanisms of the multilayer composite films, and should be of broad relevance to improve the mechanical integrity of layered oxide/polymer composite materials.

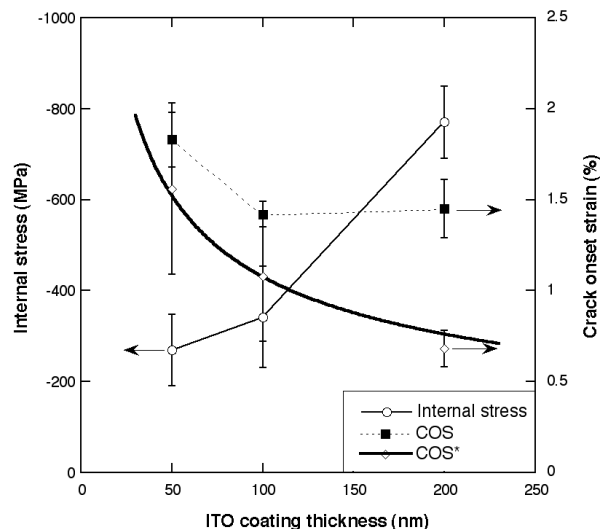


**Figure 7.** Coating thickness dependence of internal stress, measured crack onset strain (COS) and intrinsic crack onset strain ( $\text{COS}^*$ ) of as-grown ITO coatings. The thick continuous line is a power-law fit to the intrinsic crack onset strain data.

## CONCLUSIONS

Process optimization of oxide/polymer multilayer films developed as permeation barrier and transparent conductive materials for flexible displays require detailed understanding of their mechanical properties. To this end, bending tests, and tensile tests in-situ in a microscope, both equipped with resistance measurements were designed and used to analyze  $\text{Al}_2\text{O}_3$ /acrylate based barrier films, and ITO based conductive films, both deposited on a hard coat/polyester substrate. The two test methods provide accurate and identical determination of failure strains. The bending test is fast but limited to conductive coatings, whereas the tensile test enables detailed insight into failure processes in the thin layers.

The  $\text{Al}_2\text{O}_3$  layer is under limited internal compression and its crack onset strain is equal to 0.75%. The corresponding minimum achievable radius of curvature is equal to 7 mm. The adhesion of the  $\text{Al}_2\text{O}_3$  to the hard coat is higher than that to the acrylate, although complex mechanical coupling phenomena resulting from the failure of the hard coat prevent accurate determination of adhesive strength. Numerical analysis of the barrier structure is required to overcome this drawback.

The ITO layers are under significant levels of compressive stresses, and their behavior is thickness dependent. The strain to failure combines internal compression and intrinsic cohesion, which scales as the inverse of square root of ITO thickness. The minimum achievable radius of curvature for the 50 nm thick ITO coated film is close to 3 mm, and it is approx. equal to 3.5 mm for both the 100 nm and 200 nm thick ITO layers.

## ACKNOWLEDGEMENTS

The authors are indebted to the IST program (IST-2001-34215 FLEXled) for funding this work. They acknowledge the companies Ferrania, Vitex Systems and Unaxis Displays for the supply of the films samples.

## REFERENCES

- [1] Forrest S., Burrows P. and Thompson M., "The Dawn of Organic Electronics", *Ieee Spectrum*, **37**, 29 (2000).
- [2] Letierrier Y., "Durability of Nanosized Gas Barrier Coatings on Polymers", *Prog. Mater. Sci.*, **48**, 1 (2003).
- [3] Cairns D.R., II R.P.W., Sparacin D.K., Sachsman S.M., Paine D.C., Crawford G.P. and Newton R.R., "Strain-Dependent Electrical Resistance of Tin-Doped Indium Oxide on Polymer Substrates", *Appl. Phys. Letters*, **76**, 1425 (2000).

- [4] Chen Z., Cotterell B. and Wang W., "The Fracture of Brittle Thin Films on Compliant Substrates in Flexible Displays", *Eng. Fract. Mech.*, **69**, 597 (2002).
- [5] Fortunato E., Nunes P., Marques A., Costa D., Aguas H., Ferreira I., da Costa M.E.V., Godinho M.H., Almeida P.L., Borges J.P. and Martins R., "Influence of the Strain on the Electrical Resistance of Zinc Oxide Doped Thin Film Deposited on Polymer Substrates", *Advanced Engineering Materials*, **4**, 610 (2002).
- [6] Suzuki S., Hashimoto N., Oyama T. and Suzuki K., "Effect of Internal Stress on Adhesion and Other Mechanical Properties of Evaporated Indium Tin Oxide (ITO) Films", *J. Adh. Sci. Technol.*, **8**, 261 (1994).
- [7] Matthewson M.J., Kurkjian C.R. and Gulati S.R., "Strength Measurement of Optical Fibers by Bending", *J. Am. Ceram. Soc.*, **69**, 815 (1986).
- [8] Bouten P.C.P., "Failure Test For Brittle Conductive Layers On Flexible Display Substrates", *Proc. Eurodisplays, Nice (F)*, Oct. 1-4, SID, 313 (2002).
- [9] Leterrier Y., Boogh L., Andersons J. and Månson J.-A.E., "Adhesion of Silicon Oxide Layers on Poly(Ethylene Terephthalate). I: Effect of Substrate Properties on Coating's Fragmentation Kinetics", *J. Polym. Sci. B. Polym. Phys.*, **35**, 1449 (1997).
- [10] Röhl K., "Analysis of Stress and Strain Distribution in Thin Films and Substrates", *J. Appl. Phys.*, **47**, 3224 (1976).
- [11] Leterrier Y., Wyser Y. and Månson J.A.E., "Internal Stresses and Adhesion of Thin Silicon Oxide Coatings on Poly(ethylene Terephthalate)", *J. Adhes. Sci. Technol.*, **15**, 841 (2001).
- [12] Izumi H., Adurodija F.O., Kaneyoshi T., Ishihara T., Yoshioka H. and Motoyama M., "Electrical and Structural Properties of Indium Tin Oxide Films Prepared by Pulsed Laser Deposition", *J. Appl. Phys.*, **91**, 1213 (2002).
- [13] Hu M.S. and Evans A.G., "The Cracking and Decohesion of Thin Films on Ductile Substrates", *Acta Metall.*, **37**, 917 (1989).
- [14] Kim S.-R. and Nairn J.A., "Fracture Mechanics Analysis of Coating/Substrate Systems: I. Analysis of Tensile and Bending Experiments", *Eng. Fract. Mech.*, **65**, 573 (2000).